

MECHANO-CHEMICAL ACTIVATION OF KAOLIN MINERALS

ZOLTÁN JUHÁSZ

ABSTRACT

Tests have been made to study processes during the intensive grinding (supergrinding) as mechanical activation of kaolins. Activation was made by dry grinding for different times in a vibrating mill. Conclusions:

1. Change of the inner morphology of kaolin powders is due to three partial processes: disintegration, aggregation and agglomeration. The first one prevails for a short activation time, the latter two being overwhelming in prolonged activation. Therefore the grade of dispersity initially grows to decrease after prolonged grinding. In this latter case, compacted aggregates result, inaccessible to soaking in water, even if a peptizer is added. Also plasticity of the kaolin-water system decreases.

2. Supergrinding also affects the mutual adhesion, adsorption properties and action exchange capacity of kaolin particles as well as the acid solubility of kaolins very much. Test data hint to surface activation. At the same time, surface active centres will be covered by neighbouring particles ("overlapping effect").

3. Supergrinding causes amorphization of the crystal structure, beside appearance of fireclay structure. Amorphization is bound to a critical crystallite size, and has different rates along each crystallographic direction.

4. Destruction of the crystal structure of kaolinite is concomitant to the release of water of structural OH groups followed by incorporation of water into a gel structure. Xerogel when heated yields stable phases at the same high temperature as the original kaolinite. The high-temperature sintering process is, however, somewhat different in the two materials.

5. Mechano-chemical processes are somewhat accessible to artificial influencing by preliminary ion exchange.

INTRODUCTION

"Mechanical activation" is understood as to increase the free energy of solid systems by mechanical effects, changing the inner morphology of solids e. g. reducing the particle size of dispersed systems, or increasing the specific surface by deformation. But the crystal structure may also be modified, e. g. deformed, the number of lattice defects may increase, even degree of crystallinity may decrease. This latter case of changes affecting chemical bonds is referred to as "mechano-chemical activation" often accompanied by polymorphic transformations and chemical reactions [JUHÁSZ, 1974].

The simplest way of mechanical activation is grinding. Mechanical activation is conditioned by an equipment providing very intensive grinding e. g. in vibrating or ball mills for a very long time, referred to as "supergrinding".

In the following, morphological and structural changes in kaolin supergrinding will be considered. Research has been governed partly by practical, and partly by theoretical aspects. Practical aspects included determination of quality changes in kaolin grinding, and of the effect of kaolin sample preparations (pulverization) on

material testing results; theoretical research concerned causes of these phenomena. The recognized processes may be assumed to be of importance for the development and further transformations of natural kaolins, in conformity with the given geological conditions and outer mechanical effects.

SURVEY OF PUBLICATIONS

The phenomenon of kaolin crystallinity loss after prolonged grinding has long been known. KELLEY and JENNEY [1936] reported transitory widening of X-ray lines, followed by complete decomposition of the crystal structure after prolonged grinding, a statement confirmed by several subsequent investigations.

Owing to the fact that grinding is of high importance for the preparation technology of kaolin minerals, and application in ceramics, many research has obviously been spent on morphological and structural changes due to wet and dry grinding [KÖHLER, 1960; WIEGMANN, 1957; SHAW 1942; PERKINS, 1948; HAASE, 1959]. According to these investigations structural transformations are moderate or missing while particle size reduction is important upon wet grinding of kaolins. On the other hand, in dry grinding, crystal structure is destroyed, amorphization is, however, accompanied by a slight particle size reduction. In this latter case, prolonged grinding may even be accompanied by a decrease of the specific surface [AKAMATU, 1965; JUHÁSZ, 1969]. Aggregates responsible for the decrease of the specific surface are assumed to have a structure like a Hofmann-type house of cards [KÖHLER, 1960].

Destruction of the kaolin structure in grinding has been experimentally demonstrated by thermal analysis, X-radiography and IR absorption methods [HLAVAY, 1976]. As a rule a disordered crystal structure arises first, passing into a fully amorphous one after prolonged grinding. SCHRADER *et al.* [1970] comprehensively investigated mechano-chemical transformations of the kaolin structure. Increasing the grinding time, the particle size decreased (slightly) along the *c* axis, but rather rapidly and significantly did so along the *b* axis, causing kaolin to loose its lamellar habit. At the same time crystal structure was deformed mainly along the *c* axis, being more resistant along the *b* axis. In an intermediate phase of transformation kaolinite passes into a fireclay structure.

Several authors have observed appearance of fireclay structure in grinding [LAWS, 1946; WIEGMANN, 1957; JUHÁSZ, 1969].

LEHMANN [1955] observed a DTA-curve like that of illite, MILLER [1970] reported on a phenomenon of fast prototropy.

Also modification of cation exchange capacity and adsorptivity upon grinding of kaolin may be explained partly by the increase of specific surface, and partly by changes of the crystal structure. Cation exchange capacity is normally increasing or follows a maximum curve *vs.* grinding time [GREGG, 1954; KÖHLER, 1960; SANYAL, 1961; BARTHOLOMÄ, 1960; JUHÁSZ, 1969]. Increase of water adsorptivity and of adsorption energy refers to the increase of surface active energy of kaolin crystals [HAASE, 1959], and so does the increase of the activity of kaolin catalysts [AKAMATU, 1965] and that of the methylene blue adsorptivity [BARTHOLOMÄ, 1960].

The combined effect of crystal structure amorphization and of the specific surface increase may be responsible for the increase of kaolin solubility after grinding [OCEPEK, 1966]. BARTHOLOMÄ and SCHWIETE [1960] stated the total Al, Fe, Na, K and Ca to be dissoluble from sufficiently activated kaolin using dilute hydrochlorid acid, the residual being practically pure silica gel. According to GREGG *et al.* [1954], solubility monotonously increases with the grinding time, while the specific surface

varies according to a maximum curve, ascribing the increase of solubility not only to the increase of active surface but also to the decrease of crystal stability.

In general, wet grinding has been observed to improve, and dry grinding to impair the plastic properties of kaolin [KÖHLER, 1960], although some improvement is possible in the initial stage of dry grinding. This is why wet grinding is preferred to dry one for ceramic kaolin.

No uniform views have developed concerning firing properties after grinding. Sintering seems to be primarily affected by the particle size rather than the degree of amorphization [HILLER, 1968]. LÖCSEI [1970] ground kaolinite with 13% of AlF_3 and then heated it. More mullite has developed in heating, at a lower temperature (650 °C). Grinding is likely to favour metakaolin → spinell transformation, just as high static pressure [BLAIR, 1972].

After mechanical activation, reactivity of kaolin to CaO was found to increase greatly. MEHTA [1971] made cement from superground kaolin — mixed with lime — without thermal energy utilization. Direct chemical reactions were found to occur during the combined grinding of kaolin and CaO.

RESEARCH METHOD

Our tests involved kaolin samples of different origin, with symbols, oxide and mineral compositions compiled in Table 1. Mechanical activation of kaolin samples pre-ground to below 60 μm was made in a laboratory vibrating mill type KEFAMA containing 2-litre grinding pans. Materials with different activities were produced by varying the grinding time (vibration amplitude of the mill was 2 mm, at a frequency of 1300/min; charge: 60 g of sample, and 2100 g of steel balls \varnothing 2 to 10 mm).

Activated materials have been examined from the following aspects:

- powder morphology;
- particle surface texture;
- crystal structure;
- aqueous suspension properties and
- heating behaviour.

TABLE 1

Oxide and mineral composition of the samples

Symbols: Occurrences:	SzK Szegi	SzF Szegi	SK Sárisáp	HK Mád-Her- cegköves	ZK Sedlec (Zettlitz)
SiO ₂	46,1%	49,0%	60,5%	47,8%	45,6%
Al ₂ O ₃	34,2	31,6	27,5	37,3	37,0
Fe ₂ O ₃	3,24	3,24	1,12	0,31	1,10
CaO	0,65	0,70	0,66	0,10	1,10
MgO	0,68	0,65	0,26	0,05	0,10
K ₂ O	0,10	0,12	0,61	0,01	0,78
Na ₂ O ₃	0,07	0,10	0,10	0,01	0,30
H ₂ O	14,85	13,97	8,75	13,91	14,5
Kaolinite minerals:	92	95	63	92	87
	(kaolinite)	(fireclay)	(kaolinite)	(dickite)	(kaolinite)
Illite	3	—	9	—	7
Montmorillonite:	—	—	—	4	—
Quartz:	4	5	26	4	6

CHANGES IN THE INNER MORPHOLOGY OF POWDERS

From the aspect of inner morphology, in the aggregation structure of a powder — e. g. of kaolin — three parts may be distinguished:

1. Solid skeleton, bulk of primary kaolin crystal particles as an independent phase (solid part of the dispersed system).
2. Pore system: primary particles normally join secondary particles accommodating open and closed pores, capillaries, voids, possibly cracks composing a pore system dispersed throughout the aggregation.
3. Void system: coherent particle interstices in the loose powder aggregation.

Accordingly, as a first approximation, inner morphology of powders may be described in three different ways:

Volume percentages

In a bulk of 1 ml, volume ratios of solids, pore system and void system are compactness ξ , porosity ε and voids ratio κ , respectively:

$$\xi = \frac{\rho_H}{\rho}; \quad \varepsilon = \frac{\rho_H}{\rho_T} - \frac{\rho_H}{\rho}; \quad \kappa = 1 - \frac{\rho_H}{\rho_T}$$

(ρ = density, ρ_T = particle density, and ρ_H = aggregation density).

Accordingly, morphological state can be represented in the state diagram of compactness, porosity, voids ratio [in the TPH system; JUHÁSZ, 1978].

Particle porosity (in a theoretically voidless system):

$$\varepsilon_0 = 1 - \frac{\rho_T}{\rho}$$

Specific surface

Specific surface reduced to 1 g of primary and secondary particles in the powder:

$$S_V = \frac{a_P + a_H}{m}; \quad s = \frac{a_H}{m}$$

a_P and a_H being interstitial surfaces between pores and primary particles, and those between voids and secondary particles, resp., m is mass of the sample. The value of S_V has been determined from the BET relationship applied on vapour adsorption isotherms, those of ε_0 and s according to our earlier published method based on the measurement of powder permeability [JUHÁSZ, 1978]. S_V is the "dispersity degree", and s the "grinding fineness" of the system.

Granulation

Grain size curves (of aqueous systems) will be presented later. Particle shape has been tested under a scanning electron microscope.

— . —

Test data of two different kaolin samples have been plotted in *Figs 1* and *2*, exhibiting two distinct periods of activation:

1. The initial period (about 0 to 12 h of grinding time) is mainly characterized by the increase of the dispersity degree — i. e., fracture, disintegration of primary particles. Both samples being *a priori* very fine, washed kaolins, the grinding fineness

hardly changed in this period of grinding. This is, however, no general phenomenon, since in the initial period the grinding fineness mostly markedly grows for most silicate minerals. This period is generally characterized by mechanical dispersion.

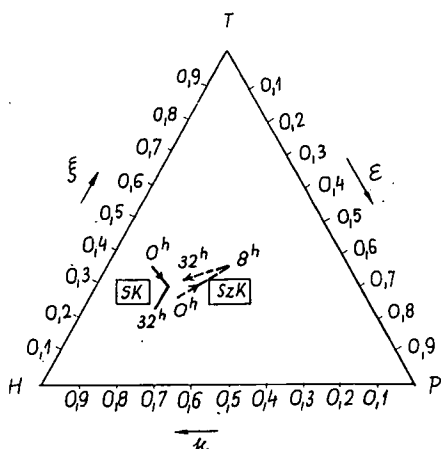


Fig. 1. Morphological changes in powders of kaolins from Sárísáp (SK) and Szegi (SzK) plotted in the morphological diagram of state compactness — porosity — voids ratio (TPH system).

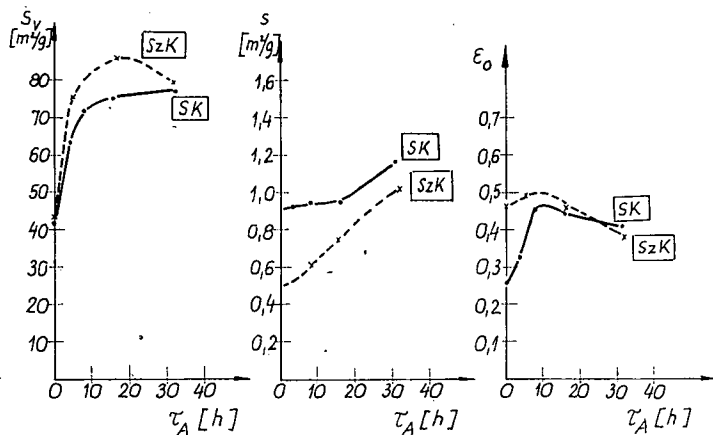


Fig. 2. Dispersity degree S_v , grinding fineness s and particle porosity ϵ_0 vs. grinding time τ_A

2. Electron photomicrographs made in the second period (after 12 h) show marked aggregation of primary particles (Fig. 3). Mechanical effect during grinding causes aggregate compaction (decreasing ϵ_0), even some pores close to become inaccessible to vapour molecules. Thereby also the specific surface S_v calculated from the vapour adsorption capacity lessens. Compact secondary particles are prone to breaking with increasing grinding time, further increasing the grinding fineness.

Thus already the powder morphology diagrams point to several partial processes in the material during kaolin activation. The following ones are of importance from morphological aspects:

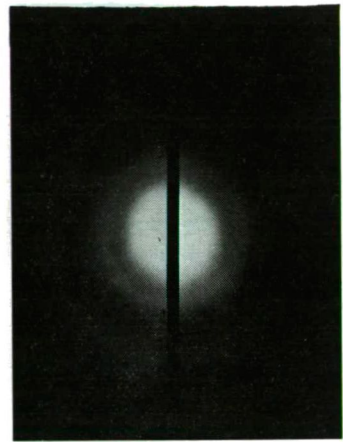
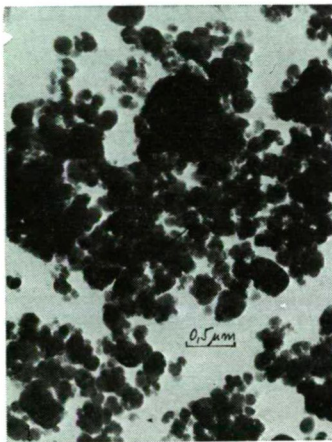
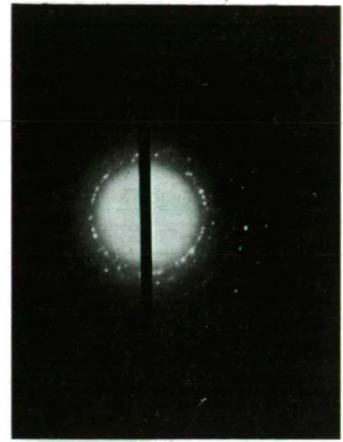
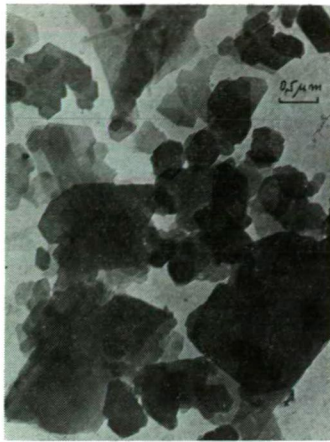


Fig. 3. Electron photomicrographs (left side) and electron diffractogram (right side) of kaolin (upper) and of kaolin-agglomerat (lower).

- Disintegration: breaking of primary and secondary particles into lesser particles. Nevertheless, partial processes of disintegration of primary and secondary particles may be independent of each other, e. g. the grinding fineness does not absolutely follow variations of the kaolinite dispersity degree.
- Aggregation: arise of secondary particles due to the interparticle adhesion. In the initial grinding period S_v increases while s remains constant indicating to a grinding equilibrium when the broken particles — as soon as arisen — aggregate to secondary ones. In grinding equilibrium disintegration and aggregation are of equal rate.
- Agglomeration: Aggregate compaction due to the effect of high surface forces, a process accompanied by fundamental changes of kaolin properties. Let us remind that the following partial processes of activation in a vibrating mill may be considered kaolins but also at other minerals: (1) initial increase

of the degree of dispersity of materials, (2) aggregate formation, (3) compaction (agglomeration) and (4) fracture (dispersion) of aggregates at a sufficient degree of compactness. All these partial processes of activation are discernible by electron microscopy.

PARTICLE SURFACE CHANGES

The concept of surface boundary layer is not the same as that of the geometrical surface. Namely an interstitial boundary layer involves the contacting surfaces of both phases, thus, in our case, atoms, ions and molecules of both the kaolin, the medium (e. g. air) and of the adsorbed „foreign” matter.

Structure of the surface boundary layer has been concluded from the following considerations:

1. Morphological stability of the powder voids system may be expressed by the specific energy of compaction, i. e. the external work spent to the compaction of the grist until its voids system completely disappears. It has been determined from step by step compaction and measurement of permeability, by graphic extrapolation. Morphological stability of the powder primarily depends on the adhesion forces between adjacent particles of the voids system.

2. The value of silicate surface polarity has been derived from the water adsorption potential ψ_v calculated from vapour adsorption isotherms, ψ_v is the energy released by 1 m² surface adsorbing water up to saturation. Its value has been calculated from vapour adsorption potential diagrams.

3. The cation exchange capacity (T value) has been determined by the modified Mehlich method. The cation exchange value has been reduced to 1 m² surface:

$$T' = \frac{T}{S_v} \quad [\text{mge/m}^2]$$

4. Water percentage $w_g\%$ unevaporable in air at a relative humidity vapour pressure $p_r=0,01$ and 23 °C but released at 380 °C has been determined as percentage of gel water and surface water with high bond energy, reduced to 1 m² of kaolin surface:

$$\alpha_v = \frac{W_g}{1800 \cdot S_v} \times 10^6 \quad [\mu\text{m/m}^2]$$

5. Aluminum percentages dissolved from the kaolins after 2 h of boiling in 0,1 n HCl have been determined and related to the initial (total) Al in the kaolin. Solubility for 1 m² surface:

$$l' = \frac{\text{Al}_{\text{dissolved}}}{\text{Al}_{\text{total}} S_v} \quad [\text{g/m}^2]$$

Test results have been plotted in Figs 4 and 5. The following conclusions should be pointed out:

1. In the initial period of grinding, interstitial properties of the kaolin are hardly changing. In this period — called the range of mechanical dispersion — surface properties are mainly affected by increase of the specific surface of the system and, consequently, by increase of values characterizing the surface texture, reduced to 1 m² area.

2. In the second period of grinding (in case of our examples, beyond 4 to 8 h of grinding) appearance of high surface-active forces may be concluded on (range of "surface activation"). These forces are likely arising from chemical bonds disrupted in connection with the fracture of kaolinite crystals and getting to the new fracture

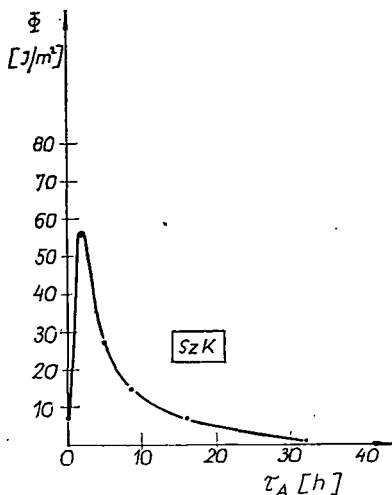


Fig. 4. Specific compaction energy Φ of powders vs. activation time τ_A

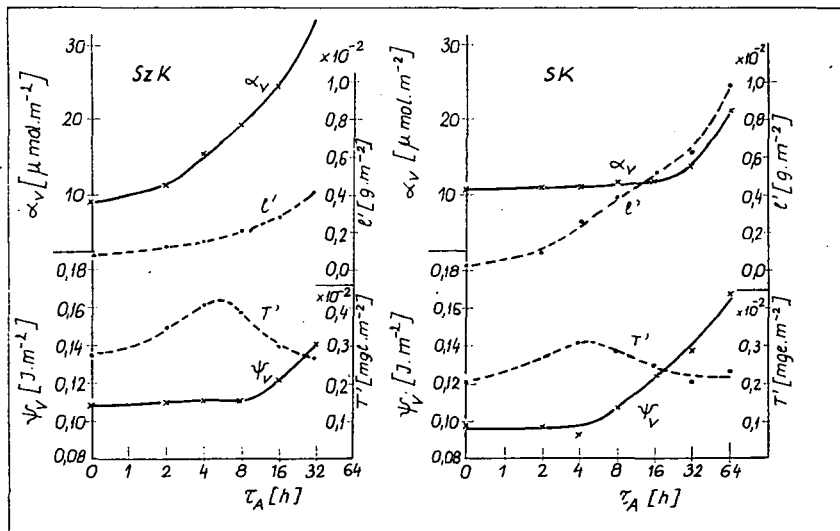


Fig. 5. Diagrams of surface texture changes

surfaces, resulting in important changes of the kaolin surface properties. They cause e. g. the increase of inter-particle adhesion i. e. morphological stability Φ of the powder, and enhance compaction inside the secondary particles (see the variation of ϵ_0).

3. Surface activation and aggregation result in the variation of cation exchange capacity according to a maximum curve. Typically, however, not only the (total) T value but also the cation exchange capacity T' related to unit area do the same. Namely, although the density of ion exchange sites initially increases on the new fracture surfaces, in a longer grinding accompanied by aggregation, part of the kaolin ion exchange centres are overlapped by neighbouring particles (apparent decrease of the surface density of ion exchange sites) to become inaccessible to exchangeable ions. This phenomenon called "overlapping effect" also appears in other silicate minerals and results, in final account, in inactivation of the surface to certain reactions e. g. ion exchange reaction. The overlapping effect is also responsible for the decrease of interparticle adhesion Φ after prolonged grinding.

CHANGES IN CRYSTAL STRUCTURE

Kaolin samples ground in a vibrating mill for different periods showed gradual transformation of crystal structure in the powder.

X-ray tests

The phenomenon will be illustrated on two different kaolins, the well crystallized kaolin of Sedlec (Zettlitz), and the *a priori* fireclay type kaolin of Szegi. (Fig. 6) X-ray diffraction patterns clearly show gradual loss of reflection intensity and appearance of an intermediate fireclay structure parallel to the degradation of the well-crystallized kaolin structure. After prolonged grinding, both kaolins transformed to X-ray amorphous materials, with practically identical diffraction patterns. From

diffraction maxima, crystallite sizes A , lattice distortion $\frac{\Delta\alpha}{\alpha_a}$ as well as the degree of crystallinity K parallel and normal to the plane of kaolinite lamellae have been calculated (Fig. 7).

Conclusions:

1. In general, crystallite sizes decreased significantly, depending on the grinding time, both normal (along the c axis) and parallel (along the b axis) to the crystal lamellae. Thus, crystallites fractured during activation. Again, the process has been observed to be speedier along the c axis than along the b axis thus, the shape of crystallites gradually changed from the anisometric, (lamellar) to the isometric one, upon adequate grinding time.

2. The lattice distortion $\frac{\Delta\alpha}{\alpha_a}$ — average deviation from the ideal lattice spacing — usually monotonously increases with the activation time.

The lattice distortion process is, however, speedier along the c axis than along the b axis (shift dislocations between and inside crystal layers). Appearance of the fireclay structure is concomitant of the disorder along the b axis.

3. Also degree of crystallinity K — referred to the initial condition as 100% — abruptly decreased with increasing grinding time, but the crystalline order in the double layers got damaged more and faster along the c axis than along the nearly normal b axis.

Thermal tests

Grinding modifies also DTA curves of kaolin as shown in Figs 8 to 10. Peak and valley temperatures $\Delta T'$ of an endothermic reaction at about 580 °C generally decrease

with increasing grinding time as shown by DTA curves of a very well crystallized kaolin (containing kaolinite and dickite), as well as by curves of medium-, and poorly-crystallized kaolins. A new reaction appears instead, at a temperature of about 150

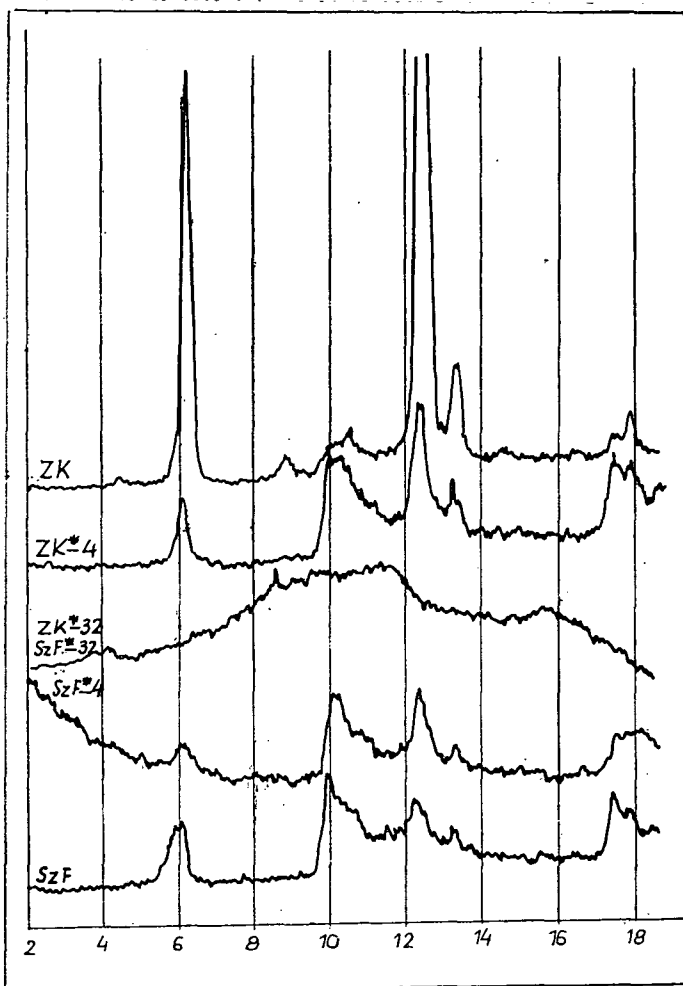


Fig. 6. X-ray diffractometric curves of kaolin from Sedlec (Zettlitz) and of fireclay from Szegi in original condition and after activation of 4 h and 32 h (activated samples marked by *)

to 200 °C. Valley depth (and area) of this latter reaction varies as a function of the activation time according to a maximum curve (Fig. 11).

“Structural water” calculated from TG curves — thus, percentage w_{OH} and activation energy E_{OH} of water leaving at 500 to 700 °C varied vs. activation time as shown in Fig. 12. Mainly upon prolonged grinding (supergrinding), mechano-chemical activation seems to cause OH groups to leave the kaolin structure, just as kaolin heated above 575 °C transformed to metakaolin. At the same time, kaolin is also

amorphized in supergrinding. (Amorphization R_{Ka} has been characterized by the mean line intensity \bar{I} of Debye-Scherrer patterns:

$$R_{Ka} = 100 - \frac{\bar{I}}{\bar{I}_0}$$

\bar{I}_0 being mean line intensity of the initial sample). This mechano-chemical decomposition of the kaolin structure reminds of the (thermal) reaction of metakaolin formation, with two differences:

— At first, activation energy of water release is different, Namely, transforming a kaolinite crystal partially into metakaolin e. g. by removing only part of the OH groups (e. g. by shorter or longer, continuous heating), upon a second heating,

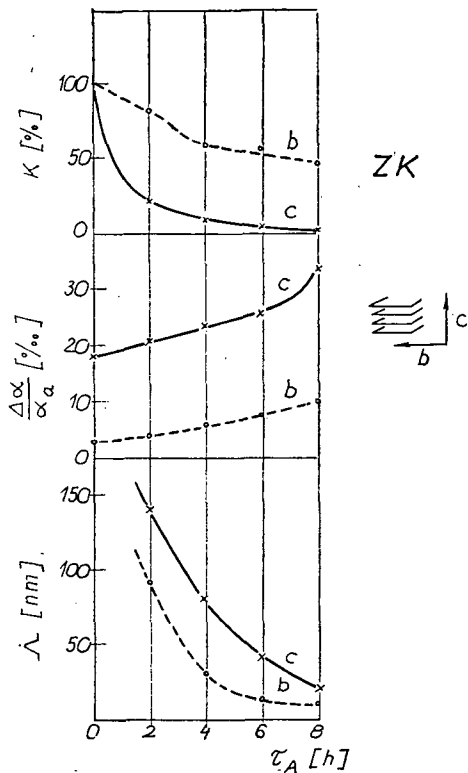


Fig. 7. Variation of crystallite size λ , lattice distortion $\frac{\Delta\alpha}{\alpha_0}$ and degree of crystallinity K of kaolin from Sedlec (Zettlitz) along crystallographic axes *vs.* grinding time τ_A

activation on energy of water representing the rest of the OH groups in higher than, or at least the same as (but absolutely not lower than), that of the water removed earlier. On the other hand, as seen in Fig. 12, activation energy of residual structural water leaving the crystal structure damaged by mechanical effects is markedly reduced, indicating the decrease of the bond energy of these OH groups.

— Secondly, while metakaolin formation is accompanied by the formation of anhydrous amorphous oxides, in mechano-chemical activation, most of the water

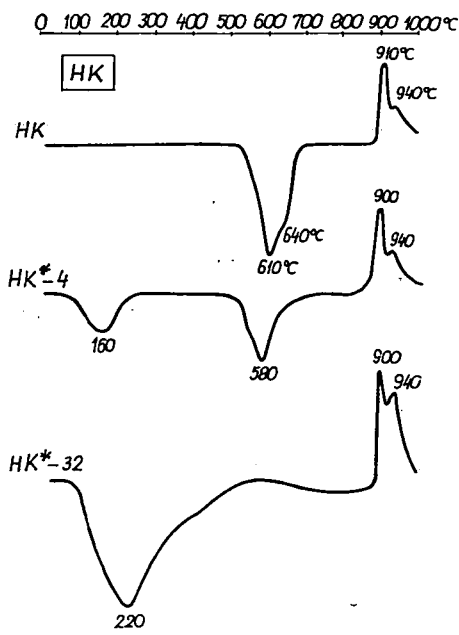


Fig. 8. DTA curves of kaolin from Hercegeköves (HK)

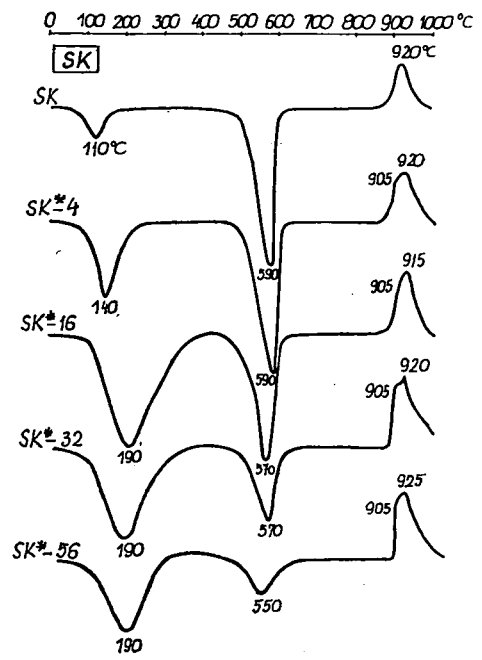


Fig. 9. DTA curves of kaolin from Sárísáp (SK)

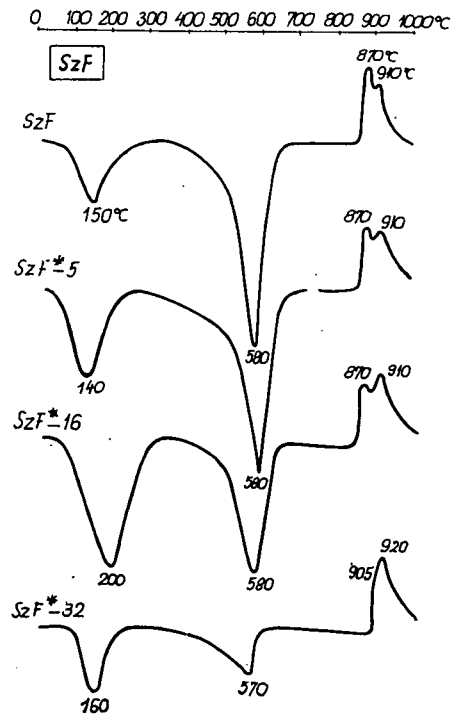


Fig. 10. DTA curves of kaolin from Szegi (SzF)

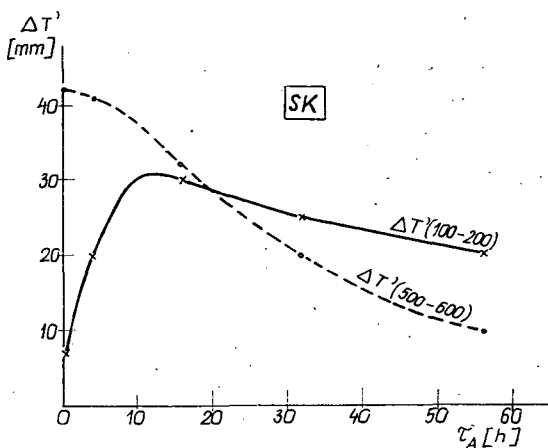


Fig. 11. First (100 to 200 °C) and second (500 to 600 °C) valley depths $\Delta T'$ of DTA curves vs. activation time

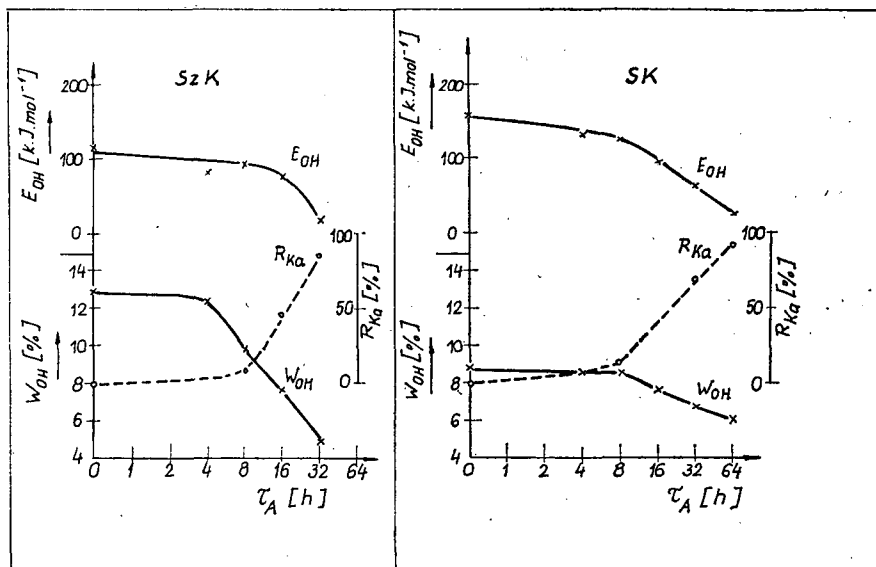
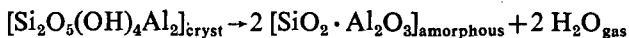


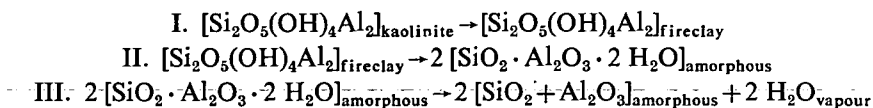
Fig. 12. Kinetic curves of the crystal structure variations of kaolins from Szegi SzF and Sárísáp SK (w_{OH} = percentage of structural water; E_{OH} = activation energy of release of structural water, R_{Ka} = amorphization of the kaolinite lattice)

leaving the crystal structure is rather strongly bound by the residual amorphous silicon and aluminium oxides as gel water. Presence of this gel water appears from endothermic maxima of DTA curves at 100 to 400 °C. Upon prolonged grinding, part of the gel water is removed.

Thus, mechano-chemical reaction of kaolinite is not identical to its thermo-chemical reaction (during heating). Thermal reaction is formulated as:



There are three steps of the mechano-chemical reaction such as



Variations in the bond of OH groups of the silicate lattice could also be demonstrated by measurements of the dielectric constant.

Dielectric tests

Dielectric constant DK of kaolins ground for different periods generally grows monotonously with the activation time (e. g. from 5 to 17). Heating these samples e. g. at 700 °C, determining the leaving water quantity and determining again the dielectric constant of the residual material cooled to 25 °C, its DK_i value will little depend on the activation time, and will be lower than that of the unheated sample (3,50 to 4,01).

Assuming the water removed by heating to be mixed with the heated material — provided no electric or chemical interaction between the water and the heated kaolin arises — calculated dielectric constant of the mixture would be:

$$DK_{\text{theor}} = v_v DK_v + v_i DK_i$$

where v_v and v_i are percentages by volume of water and solids in the mixture, and DK_v the dielectric constant of pure water.

In real silicate structures, however, water leaving upon heating is not present as an indifferent component but it is bound the silicate lattice in form of OH groups or possibly as strongly bound H_2O , hence, there is an important interaction between “water” and silicate structure. Accordingly, the dielectric constant DK of silicates is not additively composed of the dielectric constants of “structural” water and „anhydrous” kaolin, but it is lower than this theoretical value DK_{theor} . The lower it is, the stronger is the electrical and chemical interaction between the silicate lattice and OH groups or H_2O molecules in the crystal structure.

This interaction is expressed in terms of the “degree of depolarization” (ΔD_K°)

$$\Delta D_K^{\circ} = \frac{DK_{\text{theor}} - DK}{DK_{\text{theor}}}$$

(The lower is ΔD_K° , the stronger OH and H_2O are bound in the silicate structure.)

ΔD_K° values of fireclay from Szegilcng and kaolin from Sedlec (Zettlitz) have been plotted *vs.* activation time in *Fig. 13*. Degrees of depolarization of residual OH and H_2O groups monotonously decrease with activation time. Bond strength, or at least, interaction of these groups with the silicate structure is gradually reduced or at least restricted by protonation. In fireclay of originally poorer crystallinity, this process (protonization) is faster than in the well crystallized kaolin from Sedlec (Zettlitz).

Mechano-chemical test

Release of structural OH groups of kaolin, and incorporation into the xerogel structure has also been demonstrated by means of the following model test:

Gypsum previously dehydrated at 200 °C ($\text{CaSO}_4\text{-II}$) was mixed with kaolin

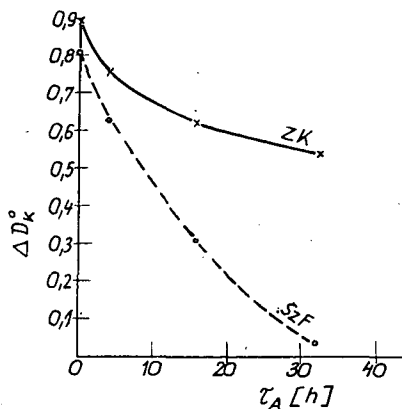


Fig. 13. Degree of depolarization of kaolin from Sedlec (Zettlitz) and fireclay from Szegi vs. grinding time. Curves point out the weakening of bond strength of OH and H₂O groups in the silicate structure

dried previously at 200 °C in a ratio of 65:35. Then mixture was ground for different times in a mill under vacuum.

Derivatographic curves were applied to calculate quantities of kaolin, gypsum hemihydrate and anhydrite in powders, shown in Fig. 14 as a function of grinding time.

Part of the anhydrite seem to be transformed to hemihydrate or dehydrate during grinding, taking the water necessary directly from the kaolin owing to the ability of a part of water to penetrate to the surrounding phase during kaolin deformation. If there is a proper counterpart (gypsum anhydrite), it will be resorbed by kaolin, however, not as structural water but as gel water bound to amorphous oxides. Thereby the amorphization of pure kaolin gets irreversible.

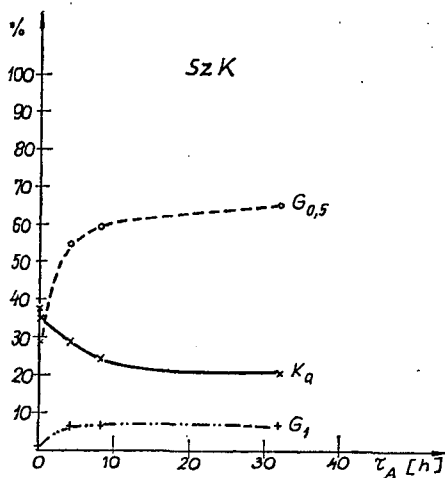


Fig. 14. Percentages of gypsum hemihydrate $G_{0,5}$ and gypsum G_1 produced by grinding of mixtures of kaolin and anhydrit, and percentage of kaolinite K_a calculated from the structural water content

Solubility-tests

Interesting information is furnished by the test of solubility on modification of the kaoline structure.

Tests have been made with hydrochloric acid in excess. Al, and Fe percentages dissolved after 2 hours of boiling have been determined and related to the total Al and Fe in kaolin (l_{Al} , l_{Fe}).

Two kinds of kaolins have been tested:

One was a relatively well crystallized limonitic kaolin from Sárísáp, the other a poorly crystallized kaolin from Szegi, peculiar by its snow-whiteness in spite of its iron content over 3% in terms of Fe_2O_3 .

Samples were exposed to two series of solubility tests: one series consisted in solving the unactivated samples in hydrochloric acid solutions of different dilutions, in the other series the acid dilution was kept constant (0,1 n) while kaolins were previously activated for different times. l_{Al} and l_{Fe} variations have been recorded (Fig. 15). The poorly crystallized kaolin SzK seems to be *a priori* more soluble than well-crystallized SK, a difference prevailing for less diluted acids. At the same time, however, increase of the dissolved Al percentage seems to be concomitant with that of Fe, but the solubility of iron from the Sárísáp kaolin increases faster than that of aluminum. In this kaolin, main mass of iron is concentrated in a well soluble separate phase (limonite), irrespective of the kaolinite solubility. On the other hand, main

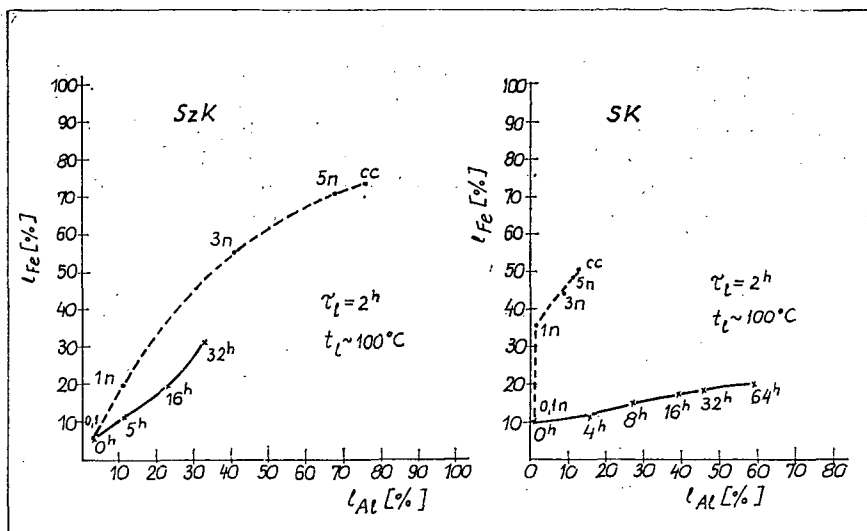


Fig. 15. Solubility of Al and Fe in kaolins from Szegi (SzK) and Sárísáp (DK) in hydrochloric acids of different n values after different grinding times

mass of iron in the kaolin from Szegi (about 80% of total Fe) is dissolved proportionally with Al. It can be calculated that about 20% of all the Al atoms are replaced by Fe atoms in the kaolinite lattice. Incorporation of Fe of high ion radius in place of Al of low ion radius results in a certain loosening of the kaolin lattice, in loss of the crystal structure stability.

After mechanical activation of both kaolins, solubilities of Al as well as of iron increase considerably. Solubility of iron l_{Fe} , however, is lower than that of alumi-

num J_{Al} . This difference is rather perspicuous for the Sárísáp kaolin, and may be ascribed to the inactivation (recrystallization, or at least, agglomeration into some inactivated nodes) of iron oxide in the mixture of amorphous oxides produced by mechano-chemical activation. The inactive behaviour of iron oxides forwards the selective solubility of aluminum.

MECHANO-CHEMICAL ACTIVATION

The above statements — in accordance with the publications — permit to state that supergrinding destroys crystal structure of kaolin and produces an amorphous xerogel. Transformation relies on the rupture of chemical bonds and arise of lower binding forces, material stability decreases and chemical reactivity increases. Therefore this way of activation affecting also the crystal structure is properly termed “mechano-chemical activation”.

In connection with mechano-chemical activation, the following has to be pointed out:

1. Mechanical activation modifies the bonding energy, since:

— new surfaces come about, increasing the specific surface of the system:

$$(S_1 - S_2) = \Delta S$$

— surface forces arising on the new surface are greater, increasing the free surface activation energy of the system:

$$E_{F1} - E_{F2} = -\Delta(E_f S)$$

(E_f being the surface potential per unit area);

— binding forces between atoms in the crystal structure, hence lattice energy of the crystal decreases:

$$E_{R1} - E_{R2} = \Delta E_R$$

Thus, overall change in the bonding energy (for 1 g of material)

$$\Delta E_K = \Delta E_R - \Delta(E_f S).$$

For the sake of simplicity — neglecting kinetic energies during grinding, heating, volume work etc. — change in the bonding energy is proportional to the change in free energy of the system:

$$k\Delta E_K = \Delta F = \Delta U - T\Delta S$$

(U =internal energy, S =entropy, k =conversion factor).

2. Three partial processes of mechano-chemical activation such as mechanical dispersion, surface activation and crystal structure changes may be independent to a degree, or at least proceed at different velocities.

This is apparent from *Fig. 16* where mechanical dispersion, surface activation and crystal structure variations have been represented as derivatives with respect to the grinding time of dispersity degree S_v , water adsorption potential ψ_v and activation energy of water release E_{OH}^0 , respectively, thus, by the variation rate of characteristics of state, and plotted as a function of activation (grinding) time (τ_A).

The presented kinetic curves show the kaolins — either poorly or well-crystallized — to be ruled initially in grinding by mechanical dispersion, the speediest process.

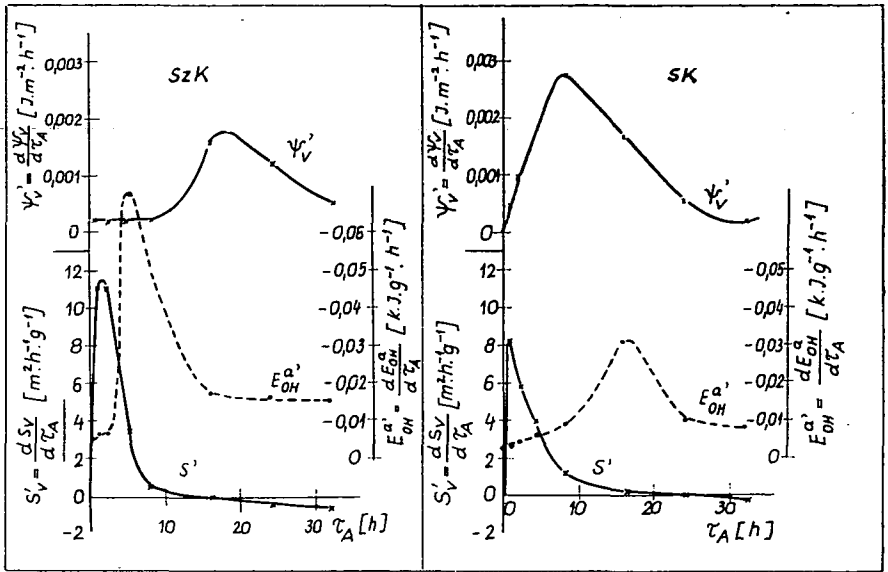


Fig. 16. Diagrams of rates of mechano-chemical activation

For sufficiently high dispersion degree, further disintegration slows down in favour of surface of crystal structure activation. The sequence is, however, variable: before surface activation the inner structure of poorly crystallized kaolin SzK gets sooner destroyed, opposite to the well-crystallized kaolin (SK).

Otherwise, various partial processes are overlapping, pointing to the statistic character of the phenomenon (activation of smaller particles precedes that of the bigger ones, a given powder may contain any particle size).

3. Amorphization is of utmost importance in mechanical activation. Fig. 17 shows degree of crystallinity to abruptly decrease with increasing specific surface.

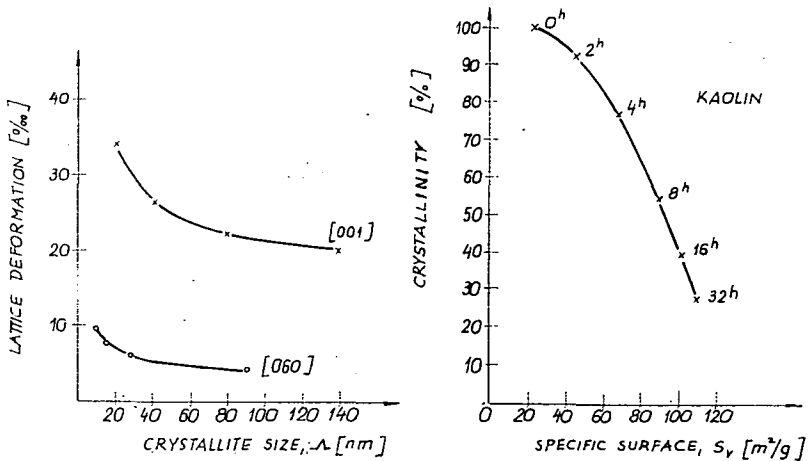


Fig. 17. Relationship between crystallite size and lattice deformation and between specific surface and degree of crystallinity.

On the other hand, with decreasing crystallite sizes, after a critical size, the lattice distortion is abruptly increasing.

This, amorphization is concomitant to the mechanical activation of adequately finely ground crystals. Below a critical size, crystals do not break up but undergo plastic deformation. As a consequence, dislocation density grows (permanently) to a degree where X-ray reflections typical of crystalline materials are replaced by an X-ray pattern typical of "amorphous" materials.

KAOLIN-WATER SYSTEMS

After mechano-chemical activation, i. e. preliminary dry grinding, of kaolins, properties of aqueous kaolin suspensions show important changes, to be described below.

Kaolin suspensions have been tested for:

- *Particle size distribution* in 2% aqueous suspension, with a Köhn—Robinson pipette. Peptizer; 2% Na_2CO_3 solids.
- *Rheology* in a rotational viscosimeter type "Rheotest 2". Suspension concentration: 24%.
- *Methylene blue adsorption specific surface*, i. e. area accessible to relatively

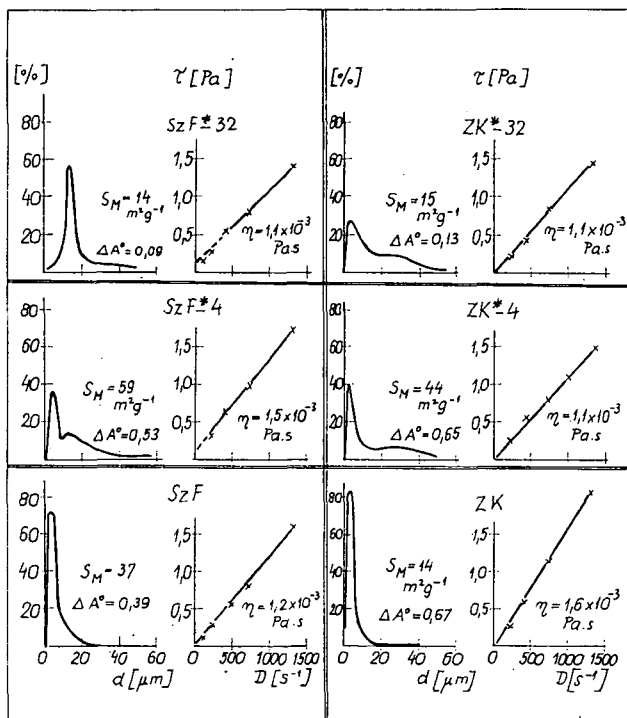


Fig. 18. Properties of aqueous solutions of fireclay from Szegi SzF and kaolin from Sedle c (Zettlitz) ZK in original conditions, and after 4 h and 32 h of activation

large-size methylene blue molecules S_M . The degree of disaggregation calculated therefrom is:

$$\Delta A^\circ = \frac{S_M}{S_V}$$

Changes of state in kaolin suspensions due to mechanical activation are shown in Fig. 18, the most important ones being:

1. Coarsening of kaolin suspensions in the activated systems due to abrupt agglomeration.

2. Coexistence of two opposite processes, i. e. mechanical dispersion and aggregation-agglomeration in the development of the methylene blue surface i. e. disaggregation degree. For instance, after 4 h of grinding, the surface S_M released in the suspension grows, but after 32 h of grinding it decreases since kaolin aggregates cannot soak, disaggregate in water. Development of the disaggregation degree, however, is a hint that the dispersity degree of the suspension is more sensitive to structural changes arising in kaolin grinding than is the "total" specific surface hence dispersity degree of the powder.

3. The above changes of the dispersity degree of aqueous systems also prevail in the evolution of rheologic properties. Mechano-chemical activation sets back the plastic properties of kaolin.

4. In addition to S_M and ΔA° , compressive strength values τ_D of kaolin-sand mixtures wet moulded then dried have been plotted in Fig. 19. "Dry strength" curve seems to follow mainly the curve of disaggregation degree, hence the maximum dry strength is achieved under the best disaggregation circumstances, possibly, in turn, at an optimum grinding time.

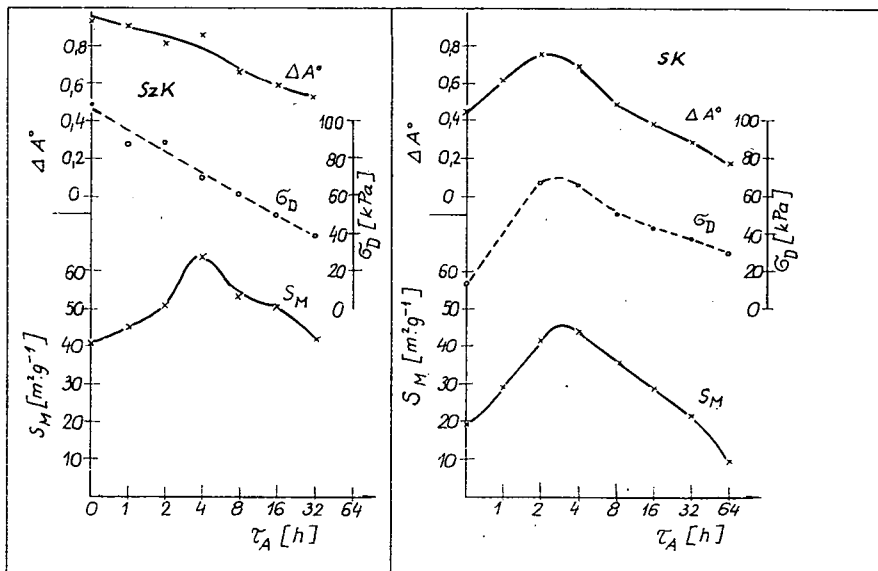


Fig. 19. "Free" specific surface S_M , degree of disaggregation ΔA° in aqueous suspensions and dry specimen strength τ_D vs. kaolin grinding time τ_A

EFFECT OF PREVIOUS CATION EXCHANGE ON ACTIVATION

Our tests pointed to a certain modification of processes in the mechanical activation of kaolins upon a previous ion exchange reaction of the kaolins with different cations.

Ion exchange was performed by evaporating kaolins with Li_2CO_3 , Na_2CO_3 and K_2CO_3 solutions, followed by suspension in water and dialytic removal of excess electrolytes.

One part of the re-exsiccated solids has been tested in original conditions. In the other part obtained after 32 h of grinding in a vibrating mill, the following characteristics were determined: vapour adsorption specific surface S_M and degree of disaggregation ΔA° , percentages of "gel water" w_g and "structural water" w_{OH} as well as activation energy E_{OH} of removal of "structural water". In addition, X-ray analysis was carried out in order to determine the phase composition F of solids ground for 32 h (Figs 20 and 21).

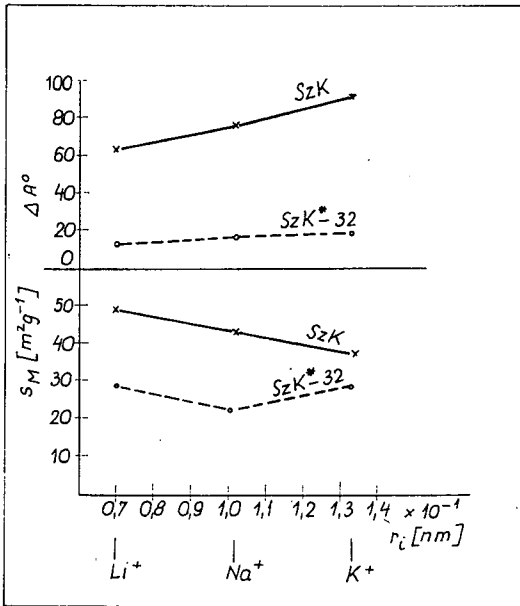


Fig. 20. "Free" specific surface S_M and degree of disaggregation ΔA° of kaolins from Szegi after ion exchange (unactivated: SzK and activated: SzK* — 32)
 r_i = Radius of the exchangeable ions

The data presented show that preliminary ion exchange may modify the properties of aqueous suspensions of unactivated or activated materials. A greater importance is due, however, to the effect of quality of cations on structural changes during mechanical activation. The strongest effect is that of Li ion (causing the maximum change of E_{OH} and the least of untransformed kaolinite). This phenomenon can be attributed to the small size of Li ions permitting them to act as local depolarizers when penetrated into the silicate structure.

The most of X-ray-amorphous material was obtained from Na-kaolin while Li- and K-kaolins produced relatively more fire-clay. In conformity with the transfor-

mation sequence kaolinite — fire-clay — amorphous, Na-kaolin seems to be transformed faster, while transformation of Li- and K-kaolins seems to be stopped at the fire-clay state.

This can be explained supposing that crystal structure transformations are influenced by the disaggregation state of kaolin (considering that both disaggregation

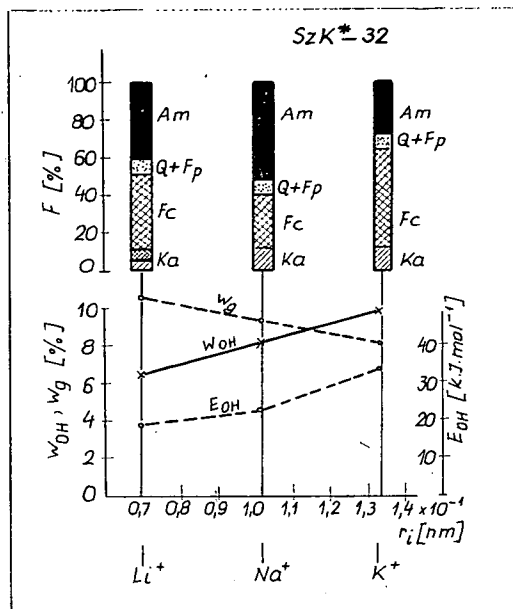


Fig. 21. Phase composition, (F%) percentages of structural water w_{OH} and gel water w_g of kaolins treated with different cations, then ground for 32 h. Activation energy E_{OH} of the release of structural water. (Am=amorphous, Q=quartz, Fc=fireclay, Ka=kaolinite)

degree and rate of crystal structure transformation of Li-kaolin are higher than those of the other two ones).

DTA curves of samples treated by different ions are shown in Fig. 22.

BEHAVIOUR UPON HEATING

Some examples will be quoted to illustrate the effect of mechanical activation on the behaviour of kaolins during heating:

1. Phase composition of kaolin heated to 1350 °C is not influenced by mechanical activation. Some effect was manifest after heating at 1000 °C, namely somewhat more corundum (a few %) formed from mechanically activated samples, the difference being, however, unimportant.

In case of kaolins where the structural water is weakly bound to the amorphous xerogel structure, high-temperature reactions are not controlled by mechanical activation since the gel water does not affect the composition of metakaolin structure preceding crystalline phase developing at high temperatures. It can be noted that

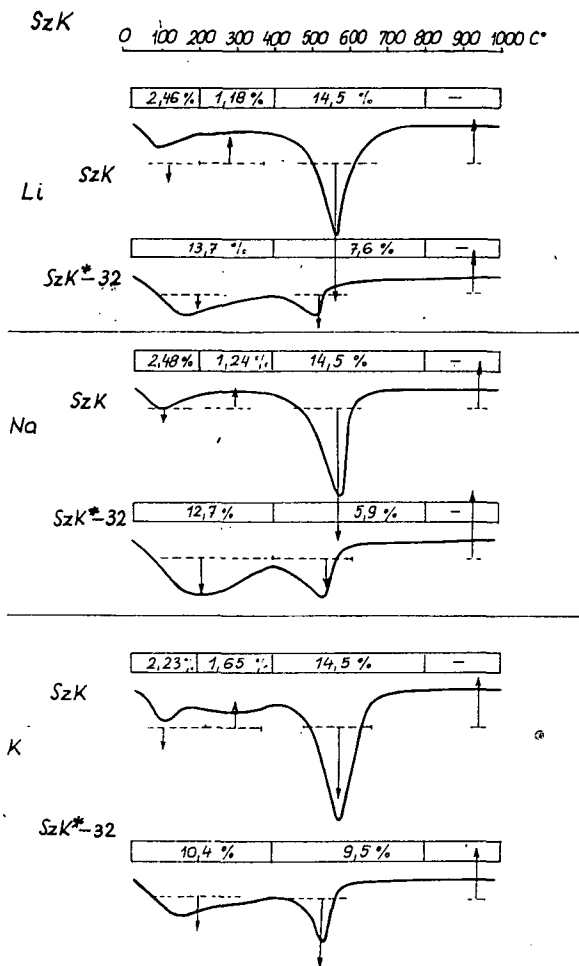


Fig. 22. DTA curves of kaolin from Szegi saturated with different cations in original condition and after grinding for 32 h; arrows indicate position and height of DTA curve maxima, number indicate mass losses

opposite phenomena were observed for other silicates such as montmorillonite, talc and pyrophyllite.

2. Upon autoclave treatment (240 °C, 96 h) of kaolin mechanically activated, the valley of DTA curves between 500 to 600 °C got deeper, and the course of the curve as a whole became the same as that of a typical fireclay mineral.

3. The effect of mechanical activation on the morphology of fired kaolin is shown in Fig. 23.

The test procedure was the following:

Kaolin from Sedlec (Zettlitz) has been tested in original condition and after 32 h of activation. The state of the grists compacted under a pressure of 10^{-1} MPa has been plotted in the morphological diagram of state compactness — porosity — voids ratio (TPH system).

Gristers were compressed under 10 MPa to specimens. Morphological changes of state may be read off the diagram.

Thereafter the specimens have been fired at 900 °C then at 1350 °C.

Final conditions at 1350 °C seem to be identical for both samples, but intermediate conditions are different. From technological aspect the most important difference may be the lower compactness of the raw specimen as compared to that of the activated specimen made under the same pressure. This difference subsisted even after being fired at 900 °C. Thus, heating from 900 °C to 1350 °C causes a greater change in the structure of activated kaolin as compared to that of the unactivated one resulting in increased shrinkage, at technologically unfavourable property of activated kaolins.

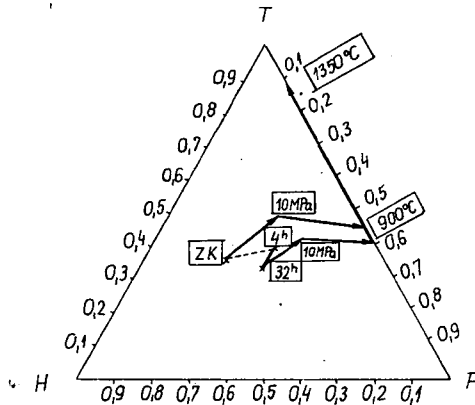


Fig. 23. Evolution of inner morphology of fired specimens pressed from kaolin powders plotted in the TPH system.

REFERENCES

- AKAMATU, H., H. TAKAHASHI [1965]: Catalytic activity of kaolin minerals. *Clay Sci.*, 5, 197—205.
- BARTHALOMÄ, M. D., H. E. SCHWIETE [1960]: Über die Mahlwirkung auf Tonminerale und den Einfluss der Oberfläche auf die Anlagerung von Ammoniumionen und Methylenblau. *Die Ziegelindustrie* 4, 97; 12, 421.
- BLAIR, G. R., A. C. D. CHAKLADER [1971]: Firing vs Reactive Hot-pressing. *J. Thermal. Anal.*, 4, 311—322.
- GREGG, S. J., K. F. HILL, T. W. PARKER [1954]: Grinding of kaolinite. *J. Appl. Chem.*, 4, 666—674.
- HAASE, TH., K. WINTER [1959]: L'influence du broyage sur les propriétés ceramiques du kaolin. *Bull. Soc. Franc. Céram.*, 44, 13—19.
- HILLER, W. [1968]: Über den Einfluss der mechanischen Aktivierung auf die Sinterung des Kaolins. *Silikattechnik* 19, 128.
- HLAVAY, J., DÓKA, I. [1976]: Porcelánmassza őrlésének és szemcseméret eloszlásának vizsgálata infravörös spektrofotometriás módszerrel. *Építőanyag XXVIII*, 197—200.
- JUHÁSZ, Z. [1969]: Szilikátásványok mechanokémiai aktiválása. *MTA Kémiai Közlemények* 31, 227—266.
- JUHÁSZ, Z. [1974]: Mechanochemische Aktivierung von Silikatmineralen durch Trocken-Feinmahlen. *Aufbereitungs-Technik*, 559—562.
- JUHÁSZ, Z. et al. [1978]: *Untersuchungsmethoden zur Charakterisierung mechanisch aktivierter Festkörper*. Budapest, KÖZDOK 1978.
- KELLEY, W. P., H. JENNEY [1936]: The Relation of Crystal Structure to Base-Exchange and its Bearing on Base-Exchange in Soils. *Soil. Sci.*, 4, 367—382.

- KÖHLER, E., V. HOFMANN, E. SCHARRER, K. FRÜHAUF [1960]: Über den Einfluss der Mahlung auf Kaolin und Bentonit. Ber. der deutsch. Keram. Ges., **37**, 493—498.
- LAWS, W. D., J. B. PAGE [1946]: Changes Produced in Kaolinite by Dry Grinding. Soil Sci., **62**, 319—322.
- LEHMANN, H., R. FAHN [1955]: Differentialthermoanalytische Untersuchungen von Kaolinen. Tonind. Ztg., **79**, 3—5.
- LŐCSEI, B. [1970]: Az őrlés hatása a kaolinit- AlF_3 reakcióra. Építőanyag XXII, 332—335.
- MEKTA, P. K. [1971]: Cement production without heat. Rock Products, May, 84—87.
- MILLER, J. G., T. D. OULTON [1970]: Prototropy in kaolinite during percussive grinding. Clays and Clay Miner., **18**, 313—323.
- OPECEK, D. [1966]: Probleme der Feinstkornzerkleinerung einiger Nichterzen. Symp. Aufbereitungs-Technik **11**, 655. (Ref.)
- PERKINS, A. T. [1948]: Kaolin and Treated Kaolins and their Reactions. Soil Sci., **65**, 185—190.
- SANYAL, J., D. LAHIRI [1961]: Wirkung der Nassmahlens auf die Korngrößenverteilung und das Basenaustauschvermögen eines unplastischen China-Clays. Trans. Ind. Ceram. Soc., **20**, 11—20.
- SHAW, B. T. [1942]: Die Natur des koll. Tones auf Grund seines Bildes im Elektronenmikroskop. J. Phys. Chem., **46**, 1032—1039.
- SCHRADER, R. *et al.* [1970]: Einfluss der Schwingmahlung auf die Eigenschaften von geschlämmten Kaolin. Silikattechnik **21**, 196—201.
- WIEGMANN, J. [1957]: Quelques observations relatives aux modifications de la kaolinite en cours du broyage. Bull. Soc. Franc. Céram., **36**, 49.

ZOLTÁN JUHÁSZ
 Department of Building Materials
 Technical University
 Műegyetem rkp. 3.
 1111 Budapest
 Hungary